phys. stat. sol. (a) **179**, 159 (2000)

Subject classification: 73.20.Dx; 73.40.Ns; S8.13

Detailed Study of Bandgap Energy Levels in CdTe Films Electrodeposited from Chlorine-Containing Solutions

A. E. RAKHSHANI[1]) and Y. MAKDISI

Physics Department, College of Science, Kuwait University, P.O. Box 5969, Safat 13060, Kuwait

(Received September 20, 1999; in revised form December 22, 1999)

Thin films of CdTe are electrodeposited at different temperatures and potentials on stainless steel foil substrates from a 1M $CdSO_4$ solution containing chlorine (0.03 to 0.06 M). Current–voltage, conductivity–temperature and photoinduced current transient spectroscopy measurements have been performed on devices formed by evaporation of semitransparent Au electrodes on CdTe. The bandgap energy levels in these films have a distinctly different spectrum compared to films deposited from Cl-free solutions. In addition to some deep hole levels which can also exist in Cl-free films, a range of shallow hole traps (within 0.4 eV from the valence band edge) have been measured and their origins have been identified. The influence of these shallow hole traps on the charge transport mechanism and the activation energy of conductivity is discussed.

1. Introduction

The conversion efficiency of solar cells made from electrodeposited CdTe can reach 14% [1, 2]. Further improvement in efficiency is closely related to the improvement of the electrical and optoelectrical properties of the material. These properties are, in particular, controlled by deep and shallow energy levels which exist in the material bandgap, due to grain-boundary and native defects, trace impurities and their complexes. Despite the extensive studies which have been done, the effects of deposition parameters, extrinsic doping and various postdeposition treatments on the spectrum of bandgap levels and, thus, on the electrical properties of CdTe, are not yet well understood.

Cadmium telluride can be electrodeposited from $CdSO_4$ solutions [3 to 7]. These films are, in general, n-type and have a high resistivity, due to the compensation effect. From the study of charge transport mechanisms in these films, it was established that a shallow donor, a deep donor-type level and a deep acceptor-type level are involved in the compensation effect [5]. The deep levels are located close to the middle of the bandgap. The presence of such deep energy levels have also been detected by photoinduced transient current spectroscopy (PICTS) in identical samples [6]. These deep levels are within two bands located about the midbandgap intrinsic level. These levels are related to the structural defects and their complexes [6] which exist within the grains or in the grain boundaries.

Electrodeposition of CdTe, for the fabrication of solar cells, was initially performed from aqueous solutions of $CdSO_4$ as described in a series of critical publications [1, 3, 7].

[1]) Corresponding author: rakhshani@kuc01.kuniv.edu.kw

Cadmium telluride can also be electrodeposited from chlorine-containing solutions of $CdSO_4$ [8 to 10]. Solar cells based on these films show a higher efficiency [11]. However, the effect of chlorine on the characteristics of CdTe films has not been discussed explicitly in these publications.

In this paper, we report on the spectrum of deep energy levels and the charge transport mechanisms in these films which are remarkably different from those in films prepared from Cl-free solutions. The present films exhibit slight p-type behavior (downward band bending when being in contact with gold) due to a lower position of the Fermi level in contrast to the upward band bending in n-type Cl-free films. Therefore, the Cl-containing films can be more suitable for the fabrication of p-CdTe/n-CdS heterojunction solar cells.

2. Experimental Details

Electrodeposition of CdTe on stainless steel 302 substrates (0.05 mm thick) was performed from a solution of 1M $CdSO_4$ (ultrapure, Alfa 20132) containing chlorine (0.03 to 0.06 M) and $HTeO_2^+$ (20 to 300 μM) at a pH = 2. Tellurium and chlorine were added in the form of TeO_2 (ultrapure, Alfa 87813) and $CdCl_2$ (ultrapure, Alfa 20887). The deposition potential was −580 to −610 mV with respect to a saturated Ag/AgCl standard electrode. The deposition was performed in the temperature range of 40 to 85 °C. The solution was electropurified for 10 to 15 h before the addition of chlorine. Films deposited for this study had a thickness in the range of 0.7 to 1.5 μm. The size of grains was estimated from the width of the XRD peaks as 40 to 50 nm. Scanning electron microscopy revealed larger grains, 100 to 300 nm size. Grains had a preferential orientation of (111) planes parallel to the substrate.

For current–voltage (I–V) measurements and the study of deep energy levels, semitransparent circular gold electrodes (14 nm thick, 2 mm diameter) were evaporated on CdTe. Positive voltage bias refers to the gold electrode being at a potential higher than the substrate.

Photoinduced current transient spectroscopy (PICTS) is a suitable technique for the study of trapping levels in high resistivity materials such as electrodeposited CdTe films [12 to 14]. This technique and the details of our measurement are described elsewhere [6]. Pulsed light (1 ms duration) from a light emitting diode (peak intensity at 637 nm) was used for excitation. The polarity of applied bias allowed the injection of either holes or electrons into the bulk of film for trapping. This method has been used successfully, in conjunction with the deep level transient spectroscopy, to distinguish between the hole and the electron traps [6, 15]. The double-gate PICTS signal which is the difference between the value of the transient current at two selected delay times peaks at a temperature, T_m at which the emission rate e_m of the trapped charge is obtainable from the selected time gates. By varying e_m through the two time gates, T_m varies according to [6, 12 to 14]

$$e_m = A\sigma T_m^2 \exp\left(-E/kT_m\right). \tag{1}$$

E and σ are the apparent energy and the apparent capture cross section of the dominant trap [6], respectively, and k is the Boltzmann constant. It should be noted that due to the possibility of thermally activated capture cross section, the apparent trap energy is greater than the actual energy by the value of the activation energy for capture cross

section; also the apparent capture cross section is the ultimate value for the cross section at high temperatures. For CdTe, $A = 1.35 \times 10^{24}\ s^{-1}\ m^{-2}\ K^{-2}$ (emission of electrons into the conduction band) or $1.07 \times 10^{25}\ s^{-1}\ m^{-2}\ K^{-2}$ (emission of holes into the valence band) [6].

3. Results and Discussion

3.1 Films deposited at 85 °C/−580 mV

The electrical properties and the effect of annealing in air on one of the samples (S25) deposited from a solution containing 0.03 M of chlorine is discussed below. Figure 1a shows, on the left side, three PICTS spectra at different rate windows for a hole trap in sample S25. The trap is identified as a hole trap since the bias used (+0.5 V) injects predominantly the holes photogenerated beneath the Au/CdTe interface, during the excitation period, into the bulk of the film where they get trapped. The T_m value shifts towards higher temperatures with increasing rate window, as expected. The related Arrhenius plot of $Y = e_m/T_m^2$ against $X = 1000/T_m$ which is expected from Eq. (1) to be a straight line, is shown in Fig. 2. This plot measures the location of the hole trap at $E_v + 0.15$ eV and its capture cross section $\sigma = 1.5 \times 10^{-19}\ cm^2$. The origin of this level is a complex defect related to Cu and/or Cl. It is well known that in bulk CdTe around $E_v + 0.15$ eV a large band of several levels exists resulting from Cu but also from V_{Cd}/Cl complexes and other impurities.

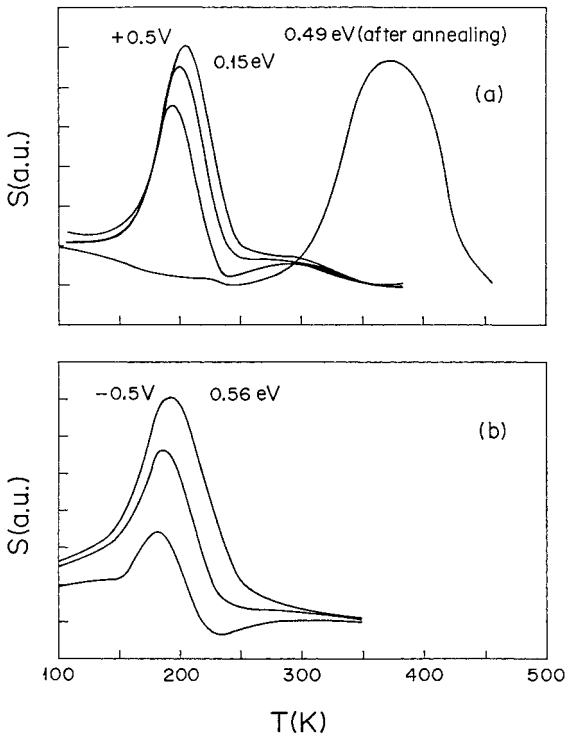

Fig. 1. Double-gate PICTS signals (S) for a 1.34 μm thick sample (S25). The bias is +0.5 V for the upper plots (part a). In the order of shifting to right, $e_m = 206$, 289 and 415 s^{-1} for the curves on the left side. The PICTS signal on the right side ($e_m = 415\ s^{-1}$) is for sample S25-A (S25 after being annealed in air at 350 °C for 30 min). The bias is −0.5 V for the lower plots (part b). In the order of shifting to right, $e_m = 96$, 144 and 482 s^{-1} for these curves. The annealed sample did not yield a PICTS spectrum with −0.5 V

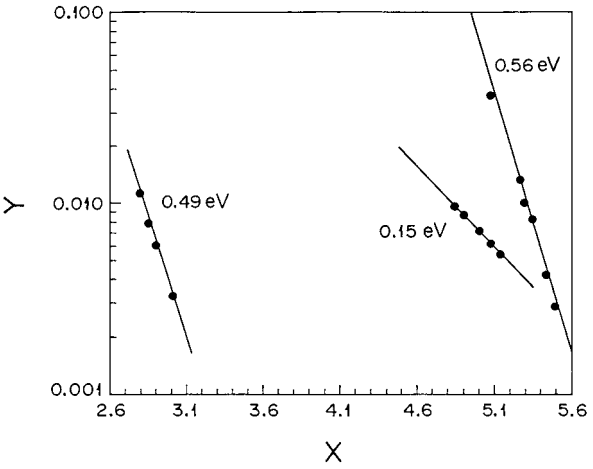

Fig. 2. Arrhenius plots of $Y = e_m^2/T_m$ (in s^{-2} K^{-1}) against $X = 1000/T_m$ (in K^{-1}) for two hole traps (0.15 and 0.49 eV) and one electron trap (0.56 eV) corresponding to Fig. 1. The energies and capture cross sections of these traps are listed in Table 1

Copper can create complexes with native defects and/or chlorine, giving rise to a band of defect levels extending from 0.11 to 0.23 eV, which leads to self-compensation of the material [16, 17]. An acceptor level at $E_v + 0.15$ eV has also been detected in a Cl-doped single crystal (p-type) of CdTe [18]. The association of chlorine with this band of defects is supported by our results which reveals that this defect band is detectable only in the present samples, but not in any of the samples deposited from Cl-free solutions [6]. It should be noted that Cu can also behave as an acceptor with ionization energy of 0.30 to 0.35 eV, by substitution into Cd sites [16, 17]. The result of our measurements on Cu-doped CdTe, electrodeposited from a Cl-free solution (not reported here) has revealed a distinct hole trap at $E_v + 0.30$ eV with $\sigma = 4 \times 10^{-21}$ cm^2. We could also detect this energy level in other samples identical to S25 which were prepared from Cl-containing solutions (see Table 1).

Figure 1a also shows a PICTS peak for a hole trap in sample S25-A which had been annealed at 350 °C in air for 30 min before gold electrodes were deposited. This hole trap is located at $E_v + 0.49$ eV, as determined from the corresponding Arrhenius plot in Fig. 2. Annealing in air replaced the $E_v + 0.15$ eV level by a much deeper level $E_v + 0.49$ eV, which is associated with cadmium vacancies (V_{Cd}^{2-}) [6]. Annealing in air also increased the short-circuit photocurrent of the sample by a few orders of magnitude. This was due to the improvement in the collection efficiency of the photogenerated carriers by the Au/CdTe contact. The PICTS spectra for an electron trap in sample S25 is shown in Fig. 1b and the related Arrhenius plot is given in Fig. 2. This trap which is located at $E_c - 0.56$ eV is possibly the same as the $E_c - 0.58$ eV level detected by DLTS (deep level transient spectroscopy) method and is likely related to a Cd_i^{2+} defect [6, 19].

The hole and electron traps measured in sample S25 and in other samples are listed in Table 1. Except for the last three samples in Table 1, all the hole traps are distinctly shallower than the hole traps in samples prepared from solutions in which chlorine was not added intentionally. For the latter samples, the ionization energy of the hole traps is greater than 0.5 eV and the Fermi level E_F is slightly above the intrinsic level E_i [6]. The shallow hole traps in the present samples apparently cause the Fermi level to be below that in n-type samples. As a result, these samples had p-type behavior. This was

Table 1

Electrical and deep levels parameters for 0.7 to 1.4 μm thick CdTe films deposited at $V = -580$ mV and $T \approx 85$ °C from different solutions. The concentration of chlorine in solution 6 and 7 is 0.03 M and 0.06 M, respectively. Solution 8 is the electropurified version of solution 7. σ is the apparent trap capture cross section and E is its apparent ionization energy. The I–V parameters ϕ, n and m are the barrier height, ideality factor and power factor, respectively. The assignement for the trap type (electron or hole) is denoted by e or h, respectively. Tentative assignments are shown in parentheses. The substrate is molybdenum for sample M51 and stainless steel for the rest. Unless otherwise stated, the bias used for PICTS measurements was 0.5 to 1.0 V with either polarities

	sample	run	solution	resistivity (Ω cm)	forward bias[a])	I–V parameters	E (eV)	σ (cm^2)	type	assignment
1	S53	1	7	5×10^5	negative	$m = 3/2$	0.11	4.5×10^{-20}	(e)	$V_{cd}^{2-}/2Cl_{Te}^{+}$ [6, 21]
2	S62	3			positive	$n = 1.37$, $\phi = 0.93$ eV	0.54	5.7×10^{-17}	e	
3	S25	4			negative	$m = 2$	0.56	2.7×10^{-8}	e	Cd_i^{2+} [21]
4	S53	1					0.67	2.0×10^{-12}	(e)	
5	S62	1	8	1×10^5	negative	$m = 3/2$	0.02	4.5×10^{-23}	h	Li, Na, P, N [6, 21, 22], O [24}
6	S62	2					0.06	1.4×10^{-22}	h	Te_i^{2-}/Cl_{Te}^{+} [25]
7	S38	2			negative	$m = 3/2$	0.11	2.7×10^{-21}	h	
8	M51	1	6	5×10^{10}	negative	$m = 3/2$	0.11	2.5×10^{-18}	h	Ag, V_{cd}^{2-}/Cl_{Te}^{+} [6, 22, 23]
9	S62	1	8				0.12	1.9×10^{-21}	h	
10	S25	2	6	1×10^8	negative	$m = 2$	0.15	1.5×10^{-19}	h	
11	S53	1					0.15	1.9×10^{-19}	(h)	Cu [21], complex defect [16, 17]
12	S53	1					0.17	1.0×10^{-19}	h	
13	M51	1	6				0.20	2.9×10^{-18}	h	
14	S25	3				$m = 2$	0.23	3.9×10^{-17}	h	GB[c])/complex defect [16, 17]
15	S62	2					0.23	1.4×10^{-19}	h	
16	M51	1					0.30	2.9×10^{-20}	h	
17	S62	2					0.30	3.1×10^{-19}	h	Cu [6, 16]
18	M51	2			negative	$m = 2$	0.35	6.6×10^{-17}	h	
19	S38	1	6	1×10^6	negative	$m = 3/2$	0.42	1.5×10^{-14}	h	GB/complex defect
20	S25-A[b])	1	6	4×10^5	positive	$n = 1.32$, $\phi = 0.94$ eV	0.49	3.3×10^{-17}	h	V_{cd}^{2-} [6, 21]
21	S38	2					0.88	4.7×10^{-8}	(h)	
22	M51	2					0.88	1.1×10^{-11}	h	Cd_i^{2+} [6, 21]
23	S53	1					0.89	2.1×10^{-12}	(h)	

[a]) Bias polarity for forward current.
[b]) Sample S25 after being annealed in air (650 K, 30 min).
[c]) Grain boundary.

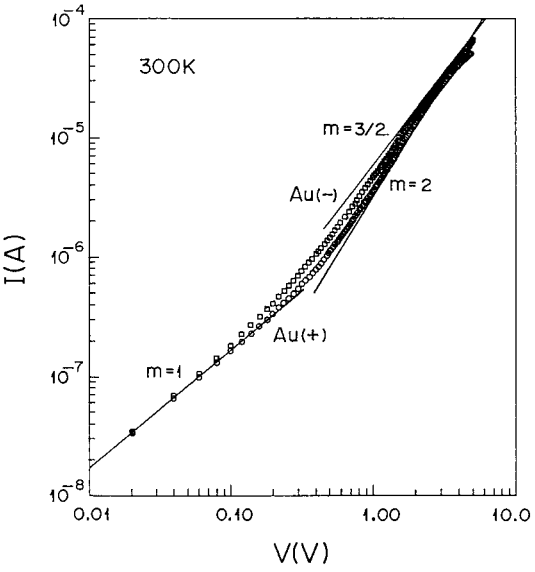

Fig. 3. Current–voltage characteristics for sample S25. The $I-V$ dependence, in both polarities, changes from Ohmic to the power law $I \propto V^m$ at a bias greater than about 0.8 V

established from the downward band bending at the gold contact. The downward band bending was determined from the easy direction of the short-circuit photocurrent. The flat-band potential varied in the range 5 to 35 mV at 300 K for different samples.

Figure 3 shows the $I-V$ characteristics in dark for sample S25. This sample does not show any pronounced rectification as for other similar samples such as S62 for which the rectification factor (ratio of forward to reverse current) was about 30 at 0.5 V. Regardless of the value of rectification factor and similar to other samples prepared from Cl-containing solutions, the forward current corresponds to a negative bias which is in accordance with the downward band bending, established from short-circuit photocurrent measurements. The forward current varies in proportion to V^m, indicating that the space-charge-limited current (SCLC) conduction is the dominant charge transport mechanism [20]. In the conventional SCLC, where conduction is controlled by discrete trapping levels, the power factor is $m = 2$. When the carrier drift mobility is field dependent, $m = 3/2$. Normally, this is the case at high fields when the drift velocity of warm carriers varies in proportion to the square root of the field [20]. $m = 2$ and $m = 3/2$ are both shown in Fig. 3 but in different bias ranges for $V > 1$ V. Inspection of Table 1 reveals that for all samples with downward band bending (forward current corresponds to negative biases) the power factor m is either 2 or 3/2. The $I-V$ plots for films prepared from Cl-containing solutions, but at deposition potentials different from those used in our samples, have shown m values in the range 2.2 to 2.4 [9]. m values greater than two are expected in cases where there is a set of trapping levels with an exponential energy distribution [20].

The $I-V$ dependence for sample S25-A is shown in Fig. 4. This is a piece of sample S25 after being annealed in air at 350 °C for 30 min. Annealing in air, which is associated with the development of a deeper hole trap (0.45 eV, as discussed above) shifts the Fermi level upward and causes an upward band bending at the Au–CdTe interface. After annealing, the forward current is associated with a positive bias and follows, in a limited range, the Schottky diode equation $I = I_0 \exp(qV/nkT)$, where the parameters have their usual meanings [5]. The ideality factor is $n = 1.22$ and the barrier height is $\phi = 0.82$ eV. From the forward $I-V$ plot which becomes linear at $V > 0.4$ V, the resistivity of the annealed film was measured as $1 \times 10^8\ \Omega$ cm which is the same as that

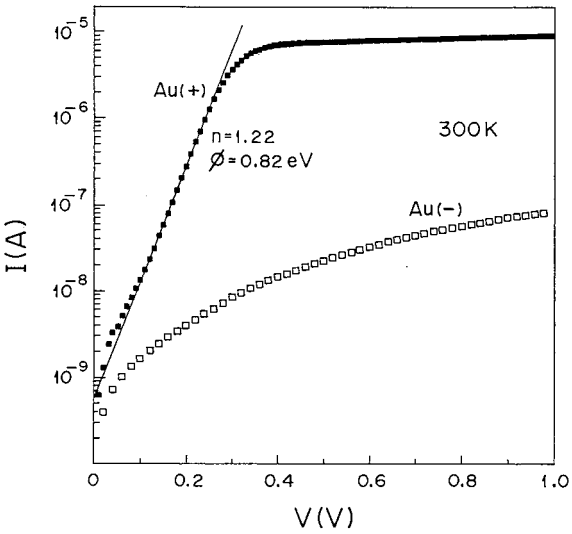

Fig. 4. Current–voltage characteristics, in both polarities, for sample S25-A (sample S25 after being annealed in air at 350 °C for 30 min). The reverse current, corresponding to a negative bias, shows the square law $I \propto V^2$ dependence on voltage for biases greater than about 0.3 V. The fit of diode equation to the forward current gives an ideality factor $n = 1.22$ and a barrier height $\phi = 0.82$ eV

before annealing. The reverse current in Fig. 4 has Ohmic behavior $(m = 1)$ for $V < 0.3$ V and SCLC characteristics $(m = 2)$ at higher voltages, similar to that before annealing.

3.2 Bandgap levels

Temperature cycling during PICTS measurement can induce changes in the deep level spectrum as a result of structural changes, migration/activation of trace impurities and formation of complex defects. Because of this, several measurements were performed on each sample and also many samples, which had been deposited from different solutions, were examined. The results are summarized in Table 1. The assignment of traps to trace impurities, native defects and their complexes was done based on the numerous published data in the literature, including [6, 16, 17, 21 to 25].

The electrical properties of a sample (S62) deposited from a solution containing more chlorine (0.06 M) showed no major differences with the electrical properties of sample S25, discussed above. This implies that the amount of chlorine that enters the film is not proportional to the concentration of chlorine in the solution, at least in the ranges used. The energy levels detected in sample S62, in different experimental runs, are listed in Table 1. The $E_v + 0.02$ to 0.06 eV is likely due to a trace impurity such as Li, Na, P, N [20, 21], oxygen [24], or/and a complex defect like Te_i^{2-}/Cl_{Te}^{+} [25]. Another level at $E_v + 0.12$ eV can be assigned to a trace impurity like Ag or to the complex defect V_{Cd}^{2-}/Cl_{Te}^{+} [6, 21 to 23]. The level at $E_v + 0.23$ eV represents a complex, or a grain boundary (GB) defect while the level at $E_v + 0.30$ eV can be assigned to Au, Ag [21] or, most likely, to Cu as discussed before. The electrical and the deep level parameters for three more samples are also summarized in Table 1.

Sample S53 is the first sample deposited from the same solution as for sample S62 (0.06 M chlorine), but before being electropurified from the trace impurities entered the solution with $CdCl_2$. This was done to examine the effect of trace impurities in $CdCl_2$ (less than 20 ppm of Au, Si, Al, Cu, Mg, Ti, as reported by manufacturer) on the

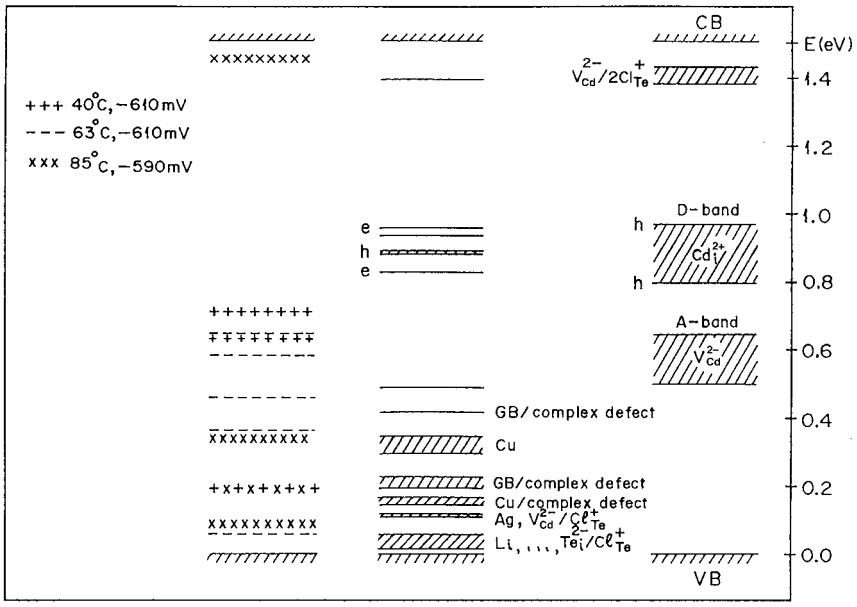

Fig. 5. Energy diagram for electron and hole traps in films deposited at 85 °C and −580 mV from Cl-free (right diagram [6]) and from Cl-containing solutions (middle diagram). The left diagram is based on the results obtained for films deposited from Cl-containing solutions (see Table 2) at −590 mV, 85 °C (× × ×), −610 mV, 63 °C (− − −) and −610 mV, 40 °C (+ + +)

spectrum of bandgap levels. Table 1 shows that all the deep levels detected in sample S53, except the Cu-related level at $E_v + 0.15$ to 0.17 eV, can be assigned to the known native defects in CdTe rather than the trace impurities in $CdCl_2$ and their complexes. The two electron traps for which their types are given in parentheses (tentative assignment) in Table 1, were measured under a low negative bias (−0.15 V) due to the experimental limitation. At low fields, the bias polarity might not be an effective mean for selecting the injection of either electrons or holes into the bulk of film and thus the type identification becomes tentative.

The spectrum of bandgap energy levels based on the results given in Table 1 and also in Table 2 (will be discussed), is illustrated in Fig. 5. This figure shows that the presence of chlorine in the bath solution with a concentration of 0.03 to 0.06 M, yields CdTe with several hole traps shallower than 0.40 eV. In addition to these levels, there are other deeper hole levels and electron levels which can also exist in films prepared from Cl-free solutions. The spectrum of energy levels in these latter films is also shown in Fig. 5 for comparison. The shallow donor band in films deposited from Cl-free solutions is attributed to traces of chlorine in solutions, as a result of contamination by the reference electrode [6].

3.3 Effect of deposition temperature

Table 2 lists the parameters of deep levels in samples deposited at different temperatures. The deposition potential could not be kept exactly the same for all. At temperatures below 85 °C, −610 mV was found to be a suitable potential for deposition of

Table 2

Electrical and deep levels parameters for three samples (thickness 0.7 to 0.8 μm, resistivity 0.1 to 10 MΩ cm) deposited at different temperatures T. The parameters and the symbols used have the same meanings as in Table 1

	sample	T (°C)	V (mV)	solution	run	forward bias[a])	I–V parameters	E (eV)	σ (cm^2)	type	assignment
1	S29	40	−610	6	1	positive	$I \propto V^2$	0.19	3.1×10^{-20}	h	GB[b])/complex defect [16, 17]
2					1			0.63	3.5×10^{-15}	h	V_{Cd}^{2-} [6, 21]
3					1			0.71	3.1×10^{-12}	h	
4	S31	63	−610	6	2	positive	$n = 1.86$, $\phi = 0.52$ eV	0.06	2.3×10^{-22}	h	Li, Na, P, N, O, Te_i^{2-}/Cl_{Te}^{+} [6, 21, 22, 24, 25]
5					2			0.36	1.1×10^{-16}	h	Cu [16, 21]
6					1	positive	$n = 1.4$, $\phi = 0.51$ eV	0.46	4.7×10^{-16}	h	GB/complex defect
7					1			0.58	3.5×10^{-15}	h	
8					2			0.63	4.9×10^{-15}	h	V_{Cd}^{2-} [6, 21]
9					2			0.64	1.9×10^{-14}	h	
10	S41	85	−590	6	1			0.05	7.4×10^{-22}	(e)	$V_{Cd}^{2-}/2Cl_{Te}^{+}$ [6, 21]
11					1	negative	$m = 3/2$	0.09	2.3×10^{-21}	h	Ag, V_{Cd}^{2-}/Cl_{Te}^{+} [6, 22, 23]
12					2	positive	$n = 1.2$, $\phi = 0.80$ eV	0.20	8.8×10^{-20}	h	GB/complex defect [16, 17]
13					1			0.34	7.6×10^{-15}	(h)	Cu [16, 21]

[a]) Bias polarity for forward current.
[b]) Grain boundary.

adherent and uniform films. On the other hand, samples prepared at 85 °C in the potential range −600 to −610 mV, were not photoconductive and, thus, sample S41 was prepared at −590 mV. The assignment of two deep levels in sample S41 (entry 10 and 13) is tentative due to the low bias (−0.1 V) used. The deep levels and the type of charge transport in sample S41 are in general agreement with those for samples prepared at 85 °C and at −580 mV (Table 1). For the other two samples (S29, S31) deposited at lower temperatures, the forward current corresponds to positive bias even in the first run, indicating an upward band bending at the gold contact. The n-type behavior of these two samples is due to the presence of some deeper hole traps (0.58 to 0.71 eV) which are in the range of A-band (V_{Cd}^{2-}) in n-type samples deposited from Cl-free solutions, as shown in Fig. 5. Electron traps could not be detected for these two samples. For these and most of other samples examined during this study, the application of a negative bias (required for the detection of electron traps) yielded noisy PICTS spectra. The n-type behavior of as-deposited samples S29 and S31 is not apparently due to the low deposition temperatures but is rather related to the deposition potentials used. Samples prepared at 85 °C but at −600 and −610 mV (not reported here) showed the same properties; the forward current, corresponding to positive bias, obeyed the Schottky diode equation. These samples, however, did not show photosensitivity. Photosensitivity could be revealed after the heat treatment of samples in air at 350 °C for 30 min. After heat treatment, charge transport mechanism changes to SCLC, but the n-type character of the samples (upward band bending) remained intact.

3.4 Activation energies

Another distinct difference between the electrical properties of CdTe deposited from Cl-free solutions (sample S2) and from Cl-containing solutions (sample S38), is noticeable in Fig. 6, in which the temperature dependence of current (in forward direction) in dark and at a constant bias is shown for both samples. Sample S2, similar to all samples deposited from Cl-free solutions (85 °C, −580 mV), shows a relatively large activation energy (0.65 eV) which corresponds to the ionization energy of an electron trap [5]. On the contrary, sample S38, like all other samples which were deposited from Cl-contain-

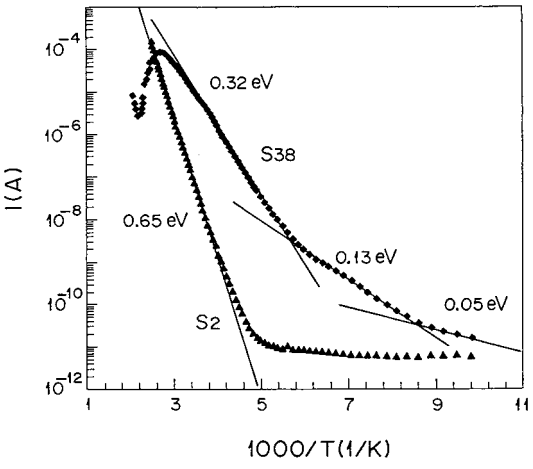

Fig. 6. Temperature dependence of forward current in dark, at a constant bias of −0.2 V for sample S38 (1.32 μm thick) and at +0.5 V for sample S2 (1.1 μm thick). The activation energies obtained from the straight line fits are 0.05, 0.13 and 0.32 eV for S38 and 0.65 eV for S2. Both samples were deposited at 85 °C and −590 mV. Sample S38 was deposited from solution 6 (Table 1) and S2 from a Cl-free solution

Table 3
The low activation energies of conductivity for films deposited from a 0.03 M Cl-containing solution at 85 °C and at different deposition potentials V

sample	thickness (μm)	V (mV)	activation energies (eV)
S38	1.32	−580	0.05, 0.13, 0.32
S25	1.34	−580	0.11, 0.20
S41	0.68	−590	0.03, 0.19, 0.25
S42	1.40	−600	0.02, 0.21
S43	1.31	−610	0.01, 0.33

ing solutions shows lower activation energies, interestingly in the range of ionization energies for the shallow hole traps determined by PICTS. Above approximately 350 K, current starts to decrease with increasing temperature and then it rises again (approximately above 450 K) showing a relatively high activation energy (≈ 0.96 eV). This behavior was observed for the majority of samples examined. The low activation energies shown below room temperature were slightly different in different samples, but remained to be less than 0.35 eV. Table 3 summarizes the low activation energies for various samples deposited at different potentials at 85 °C. The last two samples deposited at −600 and −610 mV were not photosensitive. Photosensitivity, however, could be restored by the heat treatment of samples in air at 350 °C for 30 min. The activation energy of conductivity in CdTe can be explained either in terms of the bandgap trapping levels [26] or in terms of the grain-boundary potential barriers [27]. The former seems more plausible in the light of our results which revealed a direct correlation between the shallow hole traps and the low activation energies in these samples in contrast to the deeper bandgap energy levels and the high activation energies in samples deposited from Cl-free solutions.

4. Conclusions

The Fermi energy level in CdTe films electrodeposited from Cl-containing solutions is lowered due to the influence of some Cl-related shallow hole levels. The downward shift of Fermi level causes a nearly flat band condition or downward band bending at the Au–CdTe interface. This in turn, explains the difference in the electrical properties of films deposited from Cl-containing and C-free solutions.

Acknowledgements The critical reading of the manuscript by Prof. K. Herrmann is thankfully acknowledged. The authors would like also to thank SAF for help obtained from central workshop. This work is supported by Kuwait University under research grant SP057.

References

[1] J. M. Woodcock, A. K. Turner, M. E. Ozsan, and J. G. Summers, 22nd IEEE P. V. Spec. Conf., IEEE, New York 1991 (p. 842).
[2] P. V. Meyers and R. Birkmire, Progr. Photovoltaics: Research and Applications **3**, 393 (1995).
[3] B. M. Basol, Solar Cells **23**, 69 (1988).
[4] A. E. Rakhshani and H. A. Ramazaniyan, phys. stat. sol. (a) **172**, 379 (1999).

[5] A. E. RAKHSHANI, Y. MAKDISI, X. MATHEW, and N. R. MATHEWS, phys. stat. sol. (a) **168**, 177 (1998).
[6] A. E. RAKHSHANI, phys. stat. sol. (a) **169**, 85 (1998).
[7] B. M. BASOL, J. Appl. Phys. **58**, 3809 (1985).
[8] G. C. MORRIS and S. K. DAS, Internat. J. Solar Energy **12**, 95 (1992).
[9] A. PAL, J. DUTTA, D. BHATTACHARYYA, S. CHAUDHURI, and A. K. PAL, Vacuum **46**, 147 (1995).
[10] S. K. DAS and G. C. MORRIS, J. Appl. Phys. **73**, 782 (1993).
[11] B. M. BASOL, E. S. TSENG, and D. S. LO, US Patent 4629820 (1986).
[12] D. C. LOOK, in: Semiconductor and Semimetals, Vol. 19, Ed. R. K. WILLARDSON and A. C. BEER, Academic Press, New York 1983 (p. 75).
[13] M. J. S. P. BRASIL and P. MOTISUKE, J. Appl. Phys. **68**, 3370 (1990).
[14] J. C. BALLAND, J. P. ZIELINGER, C. NUGUET, and M. TAPIERO, J. Phys. D **19**, 57 (1986).
[15] A. BLONDEEL, P. CLAUWS, and D. VYNCKE, J. Appl. Phys. **81**, 6767 (1997).
[16] M. SAMIMI, B. BIGLARI, M. HAGE-ALI, J. M. KOEBEL, and P. SIFFERT, phys. stat. sol. (a) **100**, 251 (1987).
[17] M. HAGE-ALI, B. YAACOUB, S. MERGUI, M. SAMIMI, B. BIGLARI, and P. SIFFERT, Appl. Surf. Sci. **50**, 377 (1991).
[18] C. EICHE, D. MAJER, D. SINERIUS, J. WEESE, K. W. BENZ, and J. HONERKAMP, J. Appl. Phys. **74**, 6667 (1993).
[19] W. I. LEE, N. R. TASKAR, S. K. GHANDI, and J. M. BORREGO, Solar Cells **24**, 279 (1988).
[20] M. A. LAMPERT and P. MARK, Current Injection in Solids, Academic Press, New York 1970.
[21] K. ZANIO, in: Semiconductors and Semimetals, Vol. 13, Chap. 3, Ed. R. K. WILLARDSON and A. C. BEER, Academic Press, New York 1978.
[22] T. A. KUHN, W. OSSAU, A. WAAG, R. N. BICKNELL-TASSIUS, and G. LANDWEHR, J. Cryst. Growth **117**, 660 (1992).
[23] S. SETO, A. TANAKA, Y. MASA, and M. KAWASHIMA, J. Cryst. Growth **117**, 271 (1992).
[24] K. AKIMOTO, H. OKUYAMA, M. IKEDA, and Y. MORI, J. Cryst. Growth **117**, 420 (1992).
[25] V. VALDNA, F. BUSCHMANN, and E. MELLIKOV, J. Cryst. Growth **161**, 164 (1996).
[26] CS. SZELES, Y. Y. SHAN, K. G. LYNN, and A. R. MOODENBAUGH, Phys. Rev. B **55**, 6945 (1997).
[27] R. H. BUBE, Photoelectronic Properties of Semiconductors, Cambridge University Press, Cambridge 1992 (p. 190).